Journal of Medicinal Chemistry

pubs.acs.org/jmc

Article

Synthetic Neutralizing Peptides Inhibit the Host Cell Binding of Spike Protein and Block Infection of SARS-CoV-2

Tao Wang, Xiaocui Fang, Tao Wen, Jian Liu, Zhaoyi Zhai, Zhiyou Wang, Jie Meng, Yanlian Yang, Chen Wang,* and Haiyan Xu*

Cite This: https://doi.org/10.1021/acs.jmedchem.1c01440

Read Online

ACCESS | Metrics & More | Article Recommendations | Supporting Information

ABSTRACT: Antiviral treatments of severe acute respiratory syndrome coronavirus 2 (SARS-CoV-2) have been extensively pursued to conquer the pandemic. To inhibit the viral entry to the host cell, we designed and obtained three peptide sequences via quartz crystal microbalance measurement screening, which showed high affinity at nanomole to the S1 subunit of the spike protein and wild-type SARS-CoV-2 pseudovirus. Circular dichroism spectroscopy measurements revealed significant conformation changes of the S1 protein upon encounter with the three peptides. The peptides were able to effectively block the infection of a pseudovirus to 50% by inhibiting the host cell lines binding with the S1 protein, evidenced by the results from Western blotting and pseudovirus luciferase assay. Moreover, the combination of the three peptides could increase the inhibitory rate to 75%. In conclusion, the three chemically synthetic neutralizing peptides and their combinations hold promising potential as effective therapeutics in the prevention and treatment of COVID-19.

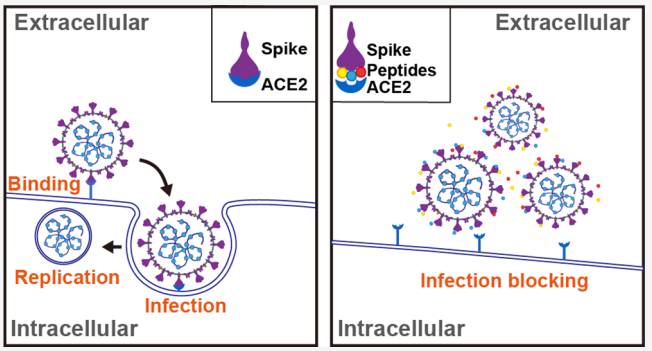

1. INTRODUCTION

An outbreak of coronavirus disease 2019 (COVID-19) caused by the severe acute respiratory syndrome coronavirus 2 (SARS-CoV-2) has widely spread worldwide. According to the WHO Coronavirus Disease dashboard, the overall mortality rate reached 2.1%.[1] The full spectrum of COVID-19 ranges from mild, self-limiting respiratory tract illness to severe progressive pneumonia, multi-organ failure, and death, which poses a serious global health emergency.[2−4] So far, there are no specific antiviral treatments available, and the lack of targeted molecular therapy for patients with SARS-CoV-2 infection has led to high mortality.[5]

SARS-CoV-2 is an enveloped, positive-sense, single-stranded RNA virus with a large genome of approximately 30,000 nucleotides in length. The virus-encoded membrane (M), spike (S), and envelope (E) proteins constitute the majority of the protein that is incorporated into the SARS-CoV-2 envelope lipid bilayer. The S protein is composed of 1273 amino acids and structurally belongs to the type I membrane fusion protein with two subunits, S1 and S2; the S1 is necessary for the host cell binding, while the S2 is necessary for membrane fusion. The S protein can form homotrimers and protrude from the envelope to show the coronal appearance, invading susceptible cells by binding angiotensin converting enzyme 2 (ACE2).[4,6]

Although several vaccines were enrolling in clinical trial and marketing[7] and conferred protection against viruses before exposure, there are still challenges to contain the COVID-19 pandemic. To bridge this gap, a therapeutic strategy for the diagnosed patients is keenly needed. Earlier efforts against COVID-19 have focused on finding out medicines for seriously ill patients, including antiviral and immune-modulating chemical compounds, such as Redemsivir that inhibited RNA replication.[8] In addition, antibody therapy has made rapid progress, and blocking the binding of SARS-CoV-2 to host cells represents one of the most promising strategies for medicine design. Since the S protein determines its binding efficiency with ACE2, it provides an important target for molecular recognition and neutralization.[9] It has been documented that antibodies for S protein could inhibit viral engagement with ACE2 and therefore could be beneficial for the treatment of COVID-19.[10−14] Convalescent plasma has been approved by the FDA for emergency use in COVID-19 patients. Moreover, several neutralizing synthetic antibodies by Regeneron (casirivimab and imdevimab or REGEN-COV)[15] and Eli Lilly (bamlanivimab and etesevimab)[16] have already been granted emergency use authorization. Single-domain antibodies were also a viable option; for instance, Chi *et al.*

Received: August 15, 2021

generated a panel of humanized single-domain antibodies (sdAbs) from a synthetic library using the receptor-binding domain (RBD) of the S protein as bait, and the sdAbs either completely block or significantly inhibit the association between SARS-CoV-2 and ACE2.[17] Since ACE2 on a cell membrane serves as a receptor of SARS-CoV-2, targeting ACE2 also represented one of the alternative strategies. A recombinant protein generated by connecting the extracellular domain of human ACE2 to the Fc region of the human immunoglobulin IgG1 could neutralize virus pseudotyped with SARS-CoV-2 spike proteins in vitro as well.[18]

Chemically synthetic peptides have a targeting function, smaller molecular weight, and are more economically costly to produce compared with antibodies or other protein-based antivirals. For example, a dimeric lipopeptide fusion inhibitor that blocks the binding step of infection and daily intranasal administration to ferrets completely prevented SARS-CoV-2 direct-contact transmission during 24 h co-housing with infected animals, under stringent conditions that resulted in infection of 100% of untreated animals.[19]

In this study, we screened and obtained three peptides and showed that each of the peptides had a high affinity to the recombinant SARS-CoV-2 S1 protein and pseudovirus of SARS-CoV-2, and hence effectively inhibited the pseudovirus with the SARS-CoV-2 S protein to bind to the host cells and blocked the infection. The inhibitory effect could be further enhanced significantly by preparing a "cocktail" with the three peptides in combinatorial experiments.

2. RESULTS AND DISCUSSION

2.1. The Peptides Showed High Affinity to the S1 Protein and Pseudovirus. In this study, a group of peptide fragments of the targeted proteins were formed in search of peptide ligands with high binding affinities (Table 1). The

Table 1. Amino Acid Sequences of the Three Synthetic Neutralizing Peptides and the Scramble Peptides with the Same Amino Acid Composition

name of peptides	amino acid sequence	purity
N1N	GDGVYYPRDVFDSSVLDSTQR	98.38%
thiolated N1N	CCPPPPGDGVYYPRDVFDSSVLDSTQR	96.58%
N1N-scramble	GGVRDYDYPVFRSSDVQLDST	98.37%
thiolated N1N-scramble	CCPPPPGGVRDYDYPVFRSSDVQLDST	98.03%
R14N	GDLFDDSNLDPFRDRISTRR	97.56%
thiolated R14N	CCPPPPGDLFDDSNLDPFRDRISTRR	97.10%
R14N-scramble	DGDLSFDNDRPLSFRITRDR	98.02%
thiolated R14N-scramble	CCPPPPDGDLSFDNDRPLSFRITRDR	98.29%
C15N	GDRIARTTRAVDRPQTLRR	97.36%
thiolated C15N	CCPPPPGDRIARTTRAVDRPQTLRR	97.15%
C15N-scramble	GRRIATDTVLRDQRAPRTR	98.25%
thiolated C15N-scramble	CCPPPPGRRIATDTVLRDQRAPRTR	96.53%

mutations and optimizations of the peptides were supported by the principles of inter-amino-acid recognition revealed by binding energies between homogeneous oligopeptides of the 20 common naturally occurring amino acids in our previous studies[20] and have been illustrated in our previous studies.[21−24]

The affinity of peptides to the recombinant SARS-CoV-2 S1 protein was quantified by the quartz crystal microbalance with dissipation monitoring (QCM-D). Specifically, peptides were thiol-immobilized onto a gold QCM-D chip by adding a CCPPPP- sequence at the N terminal. The decrease in frequency was a measure of increased mass on the surface of the chips. When the recombinant SARS-CoV-2 S1 protein was applied, the frequency of the chips decreased, indicating that the flowing S1 protein was captured by the immobilized peptides (Figure 1A). Moreover, the flowing SARS-CoV-2 pseudovirus could also be captured by the immobilized peptides (Figure 1B), which not only indicated the affinity of the peptides to the pseudovirus but also showed promising potential for rapid detection of the SARS-CoV-2 virus, for example, the peptides conjugated with iron oxide nanoparticles can be expected to act as a detecting probe with peroxidase-like enzyme activity.

The avidity index between the peptides and S1 protein was also calculated. The K_d value was calculated by fitting the saturated binding mass (Δm) as a function of peptide concentration (nM) using nonlinear regression analysis (Figure 1C−E).The K_d values of peptides N1N, R14N, and C15N were estimated to be 5.6, 37.5, and 76.9 nM, respectively. It was also shown that the peptides showed stronger binding than the scramble peptides with the same amino acid composition (Figure 1F−H).

The results of the screening process suggested three peptides that had high affinities to the recombinant SARS-CoV-2 S1 protein and pseudovirus of SARS-CoV-2. This approach could also enable the effective search for mutations and optimization of peptide segments targeting new proteins.

It is well established that the conformation or the secondary structures of proteins can be altered due to their interaction with other molecules, which may affect the protein−protein interactions. Herein, in order to investigate the structural change of the S1 protein upon introduction of peptides (N1N, R14N, and C15N), the circular dichroism (CD) spectra of the S1 protein with and without the three peptides' interaction were obtained in ddH_2O. As shown in Figure 2, the CD spectrum of S1 protein alone (black curve) in solution exhibited a maximum value near 190 nm and negative values around 210 nm, corresponding to the characteristics of mixed structures of α-helix, β-sheet, and random coils. Upon introduction of the N1N peptide (0.01, 0.1, 1, and 10 μM) into the S1 protein solution, the characteristic peaks near 190 nm were strengthened, while the characteristic peaks near 210 nm were weakened, and the positive band shifted to the left little by little, indicating that the β-sheet structure and random coils of the S1 protein gradually transformed into an α-helical structure after interacting with N1N. Meanwhile, upon introduction of R14N and C15N peptides into the S1 protein solution, the characteristic peaks near 190 nm were weakened, while the characteristic peaks near 210 nm were strengthened, and the negative band shifted to the left little by little, indicating that the α-helical structure of the S1 protein gradually transformed into random coils after interacting with R14N and C15N.

Analysis of the CD spectra using software supported the transformation of the secondary structures of the S1 protein by mixing with peptides including N1N, R14N, and C15N at different mole ratios (Table2). The percentages of the α-helix, β-sheet, and random coil structures of the S1 protein were 20, 59.4, and 20.6%, respectively. After mixing with the peptide N1N, the β-sheet structure and random coils of the S1 protein was induced into an α-helix structure, manifesting so that the percentage of the α-helical structure increased to 100%, while

https://doi.org/10.1021/acs.jmedchem.1c01440
J. Med. Chem. XXXX, XXX, XXX−XXX

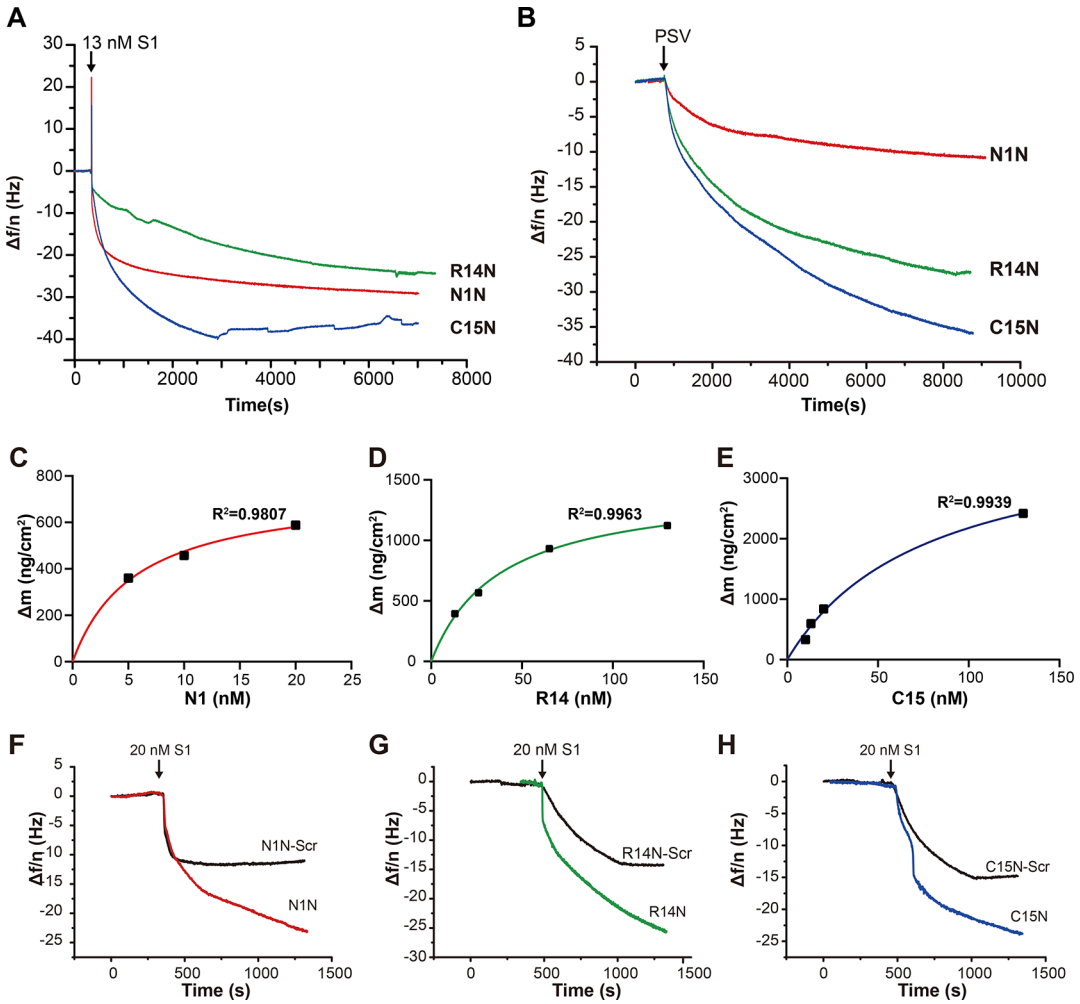

Figure 1. Peptides showed high affinity to the S1 protein. Representative QCM-D frequency variations ($\Delta f/n$) of peptide-immobilized chips when the S1 protein (A) and SARS-CoV-2 pseudovirus (B) are flowing through. Fitting curves between the variation of mass (Δm) and the peptides' concentrations (C–E). QCM-D frequency variations ($\Delta f/n$) of chips immobilized with the peptides N1N, R14N, and C15N or scramble peptides with the same amino acid composition after the S1 protein flowing through (F–H).

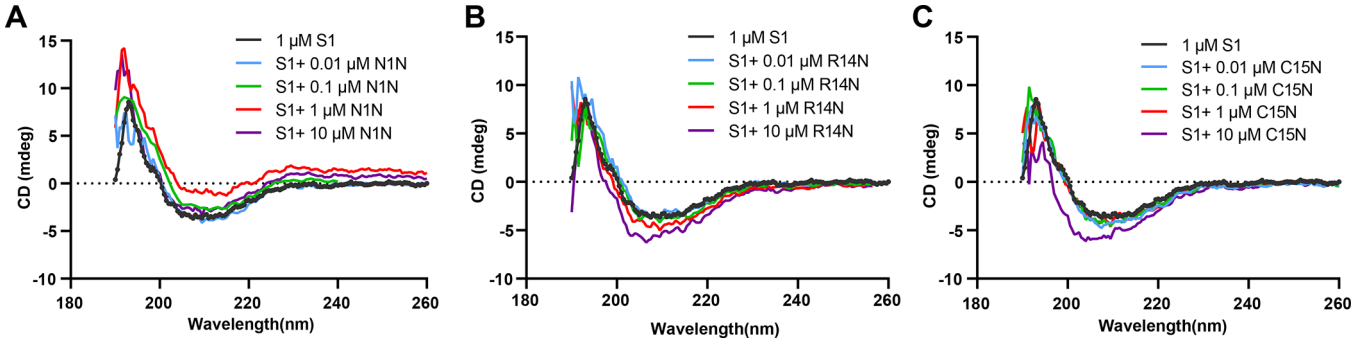

Figure 2. Conformational transformation of the S1 protein manifested by the variations of secondary structures, induced by three synthetic neutralizing peptides including N1N (A), R14N (B), and C15N (C). Every CD spectrum data used was the average of three scans and corrected for the background of the peptides and solvent.

the β-sheet structure and random coils disappeared when the mole ratio of the S1 protein and N1N was 1:0.1. Meanwhile, after mixing with the peptides R14N and C15N, the α-helical structure of the S1 protein was induced into random coils, manifesting so that the percentage of the α-helical structure decreased to 9.5 and 8.2%, while the percentage of random coils increased to 27.8 and 35.2% when the mole ratios of S1:R14N and S1:C15N were 10:1. Therefore, the CD spectra revealed that the addition of three synthetic neutralizing peptides could lead to the conformation change of S1 protein, which may inhibit the following interaction between the S1 protein and ACE2 receptors.

Circular dichroism (CD) spectroscopy is a valuable and commonly used spectroscopic technique to characterize and

https://doi.org/10.1021/acs.jmedchem.1c01440
J. Med. Chem. XXXX, XXX, XXX−XXX

Table 2. Analysis of Secondary Structures of the S1 Protein after Treatment with Three Synthetic Neutralizing Peptides

	ratio (%)											
		n (N1N):*n* (S1)				*n* (R14N):*n* (S1)				*n* (C15N):*n* (S1)			
structure	S1	0.01	0.1	1	10	0.01	0.1	1	10	0.01	0.1	1	10
helix	20	29.3	100	100	76.9	80.8	21.9	29.8	9.5	18.2	22.7	22.0	8.2
sheet	59.4	46.4	0	0	0	0	58.0	32.8	62.8	56.6	52.6	51.4	56.6
random	20.6	24.3	0	0	23.1	19.2	20.1	37.4	27.8	25.2	24.7	26.6	35.2
total	100	100	100	100	100	100	100	100	100	100	100	100	100

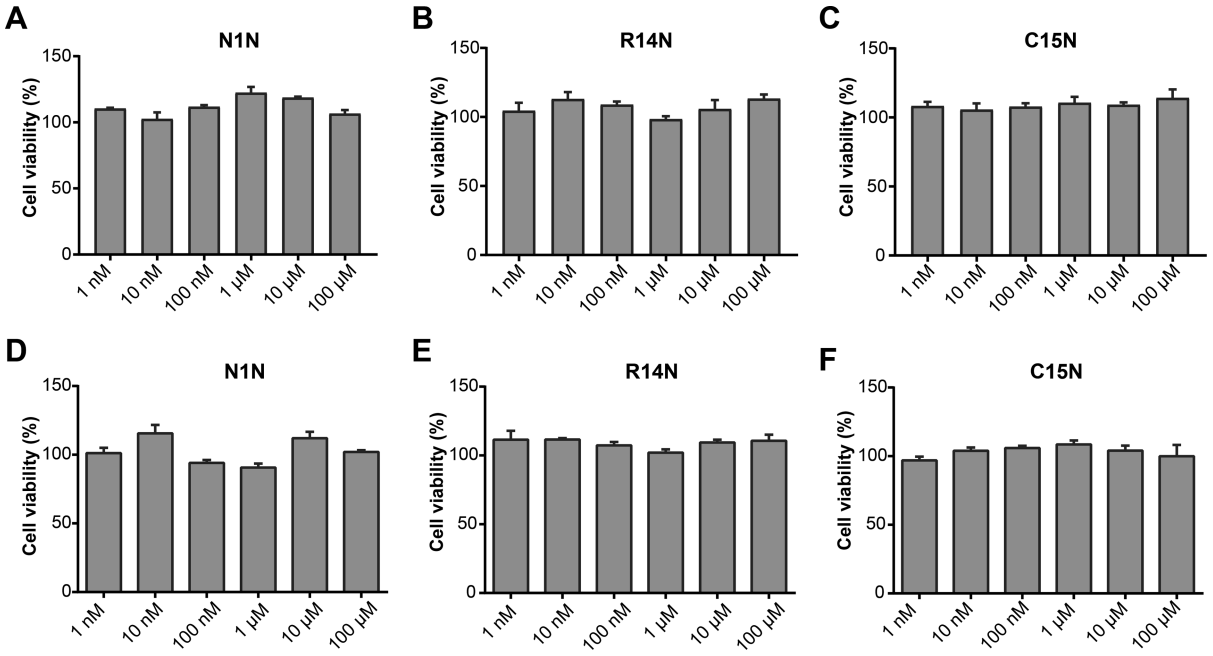

Figure 3. Relative cell viability of A549 cells (A–C) and 293 T-ACE2$^+$ cells (D–F) after being incubated with peptides N1N, R14N, and C15N for 48 h, respectively. (n = 3, data represents mean ± SEM)

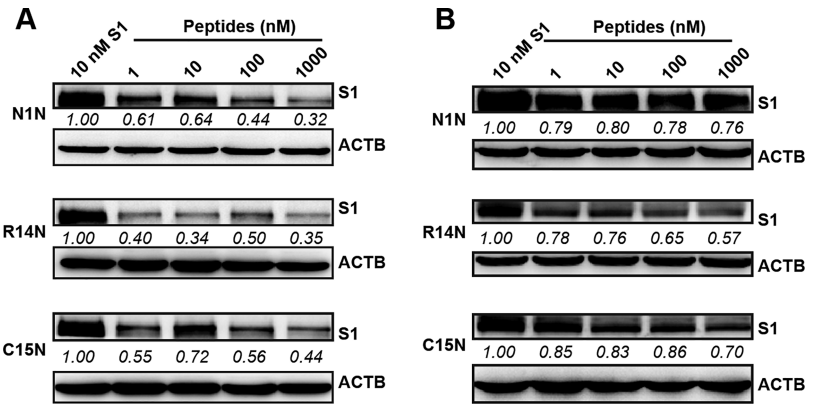

Figure 4. Peptides inhibited the host cell binding of the S1 protein on A549 cells (A) and 293 T-ACE2$^+$ cells (B).

determine the structural information of peptides in solution,[25−27] and how peptides interact with each other, so as to understand the mechanism of action.[28] It has also been used to obtain the dissociation equilibrium constant K_d of HSA with peptides in solution and detect the change of secondary structures of peptides.[29,30] In the obtained CD spectra of the peptides, no characteristic peaks can be observed. Furthermore, the CD spectrum showed that the secondary structure of the mixed solution was dominated by that of S1 protein. The observed conformational changes could be attributed to noncovalent interactions (electrostatic, hydrophobic, hydrophilic, and van der Waals) between the peptides and S1 proteins, which has been illustrated in the previous efforts on exploring allosteric effects for pharmacological applications of therapeutic ligands.[29,31] Such allosteric modulation of protein structures induced by the binding ligands is essential for the understanding of mechanisms and regulation of biological activities and has been reported in a variety of protein−ligand interactions.[32−35]

2.2. Safety Profiles of the Peptides. The cytotoxicity of the peptides on A549 cells and 293 T-ACE2$^+$ cells was examined using CCK-8 assay. After being treated with 1 nM−

https://doi.org/10.1021/acs.jmedchem.1c01440
J. Med. Chem. XXXX, XXX, XXX−XXX

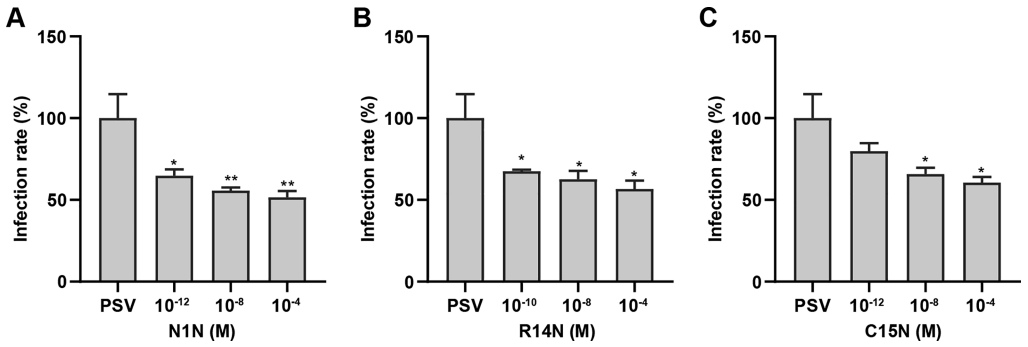

Figure 5. Infection rates of the pseudovirus (PSV) for the pre-incubation with or without peptides N1N (A), R14N (B), and C15N (C) to 293 T-ACE2$^+$ cells. *, $P < 0.05$; **, $P < 0.01$.

100 μM of peptides for 48 h, the cell viability was hardly affected for both cell lines (Figure 3), indicating that the peptides did not show any detectable cellular toxicity and suggesting that the peptides would be safe in the biological system.

2.3. The Peptides Inhibited the Host Cell Binding of the S1 Protein. Infection by SARS-CoV-2 begins with membrane fusion between the viral envelope and the host cell membrane. The fusion process is mediated by the binding between the S1 protein on the viral envelope and ACE2 on the surface of the host cells. As SARS-CoV-2 appears to mainly infect respiratory tract cells in patients,[36,37] we chose to use human pulmonary alveoli basal epithelial A549 cells as a model cell line to examine the host cell binding inhibitory effect of the peptides. Herein, the S1 protein was pre-incubated with the peptides and then applied to A549 cells. Results showed that the S1 protein bound to the A549 cells after incubation (left lane in Figure 4A), and the pre-incubation with peptides put a brake on the binding of the S1 protein to A549 cells (Figure 4A). The inhibitory effect was also observed in the well-established 293 T mammalian cell system with ACE2 overexpression (Figure 4B).

2.4. The Peptides Effectively Neutralized the Pseudovirus. The peptides inhibited the binding between the S1 protein and the host cells; we then examined whether the peptides could also block the infection of SARS-CoV-2. Herein, we utilized the pseudovirus-expressing S protein on the surface to evaluate the neutralizing effect of the peptides. The pseudovirus was pre-incubated with the peptides and then incubated with 293 T-ACE2$^+$ cells for 1 h. After that, the pseudovirus was removed and the fresh medium was supplemented. The cells were incubated for an additional 47 h. Results showed that pre-incubation with the peptides decreased the luciferase activity and the fluorescence intensity of the GFP of the cells, indicating that the peptides effectively inhibited the infection of SARS-CoV-2 pseudovirus. The infection rate was calculated according to the luciferase activity (Figure 5), indicating that the three peptides were able to inhibit the infection of SARS-CoV-2 pseudovirus to 293 T-ACE2$^+$ cells at a dose ranging from 1 pM to 100 μM. However, every single peptide could not totally inhibit the infection, probably due to the multiple sites in the spike protein that participated during the infection.

2.5. Peptide Cocktail Showed Higher Efficacy of the Inhibitory Effect. Although the three peptides could effectively inhibit the infection of SARS-CoV-2 pseudovirus, the inhibitory rate for each of them only reached about 50%. Considering that the three peptides were targeted to the different regions of the S1 protein, we applied a cocktail strategy to enhance the inhibitory effect. Results showed that the combination of the three peptides at a molar ratio of 1:1:1 (at a concentration of 10 μM) achieved a significantly higher inhibitory rate of SARS-CoV-2 infection (Figure 6), therefore providing a more effective therapeutic or preventive strategy for COVID-19.

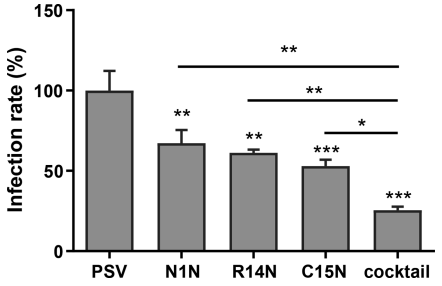

Figure 6. Cocktail of the peptides showed a more effective inhibitory effect of infection. *, $P < 0.05$; **, $P < 0.01$; ***, $P < 0.001$.

It has been documented that the RBD region in the S1 protein attributed to the binding to ACE2, and RBD-bound antibodies elicited by SARS-CoV-2 infection inhibited the viral engagement spike with ACE2, thereby blocking viral entry.[38] However, there were also antibodies against other regions of spike exhibiting neutralizing activity such as the N-terminal,[39−41] which suggested that not only the RBD domain but also the other regions of the S1 protein were essential for the infection. It is, therefore, plausible to consider that synergetic effects due to the cooperativity of multiple inhibitory interaction sites associated with the neutralizing peptides are beneficial to improve the therapeutic effects and reduce viral transmission.

Targeting viral entry in the early stages can be an effective way to treat COVID-19.[42] Due to the neutralizing effect of the peptides and safety considerations, we would suggest that both hospitalized and nonhospitalized patients could be given the peptide "cocktails" once diagnosed, which may reduce the severity and shorten the disease recovery rates. As potential therapeutics against COVID-19, the peptides can be formulated through nebulization or as dry aerosol powders for direct delivery to the lungs, and intranasal formulation may be the optimal one when using the peptides to treat COVID-19.

https://doi.org/10.1021/acs.jmedchem.1c01440
J. Med. Chem. XXXX, XXX, XXX−XXX

3. CONCLUSIONS

In this work, we have screened and obtained three peptides that were able to effectively bind to the S1 protein and SARS-CoV-2 pseudovirus, leading to the inhibition of the binding of the S1 protein and SARS-CoV-2 pseudovirus to A549 cells and 293 T-ACE2$^+$cells, therefore inhibiting the infection of SARS-CoV-2pseudovirus. Furthermore, the cocktail composed of the three peptides significantly enhanced the inhibitory effect, showing promising potential for the prevention and treatment of COVID-19.

4. EXPERIMENTAL SECTION

4.1. Cell Culture. A549 cells were purchased from the Cell Resource Center of the Chinese Academy of Medical Sciences (Beijing, China) and cultured in a McCoy-5A medium supplemented with 10% fetal bovine serum, 100 U/mL penicillin, and 100 μg/mL streptomycin. ACE2-overexpression 293T cells(293 T-ACE2$^+$) were purchased from Sino Biological (Beijing, China) and cultured in a DMEM high-glucose medium supplemented with 10% fetal bovine serum, 100 U/mL penicillin, 100 μg/mL streptomycin, and 500 μg/mL hygromycin.

4.2. Synthesis of the Peptides. The sequence of the peptides is shown in Table 1. The peptides were manufactured by the solid-phase peptide synthesis and identified as target peptides by the high-performance liquid chromatography and mass spectrometry (Guoping Pharmaceutical, Hefei, China). All peptides used in this study are >95% pure by HPLC analysis (Table 1 and Figures S1−S12).

4.3. QCM-D Measurement. Thiolated peptides were used for QCM-D measurement. The gold sensor surface was coated with the thiolated peptides by incubating with aqueous solution of the peptides at room temperature for 30 min. After coating with peptides, the gold sensors (5 MHz) were embedded in a reaction chamber, and the recombinant SARS-CoV-2 S1 protein (Sino Biological) was applied as a mobile phase at a flow rate of 300 μL/min at 37 °C in PBS.

The variation of mass (Δm) was calculated using the Sauerbrey relation:

$$\Delta m = -17.7 \times \Delta f/n, \text{ ng/cm}^2$$

The K_d value was calculated by nonlinear regression using the following equation:

$$\Delta m = \frac{[\text{conc of peptides}] + K_d}{\Delta m_{max} \times [\text{conc of peptides}]}$$

4.4. CD Spectroscopy Assay. CD measurements were performed using a spectropolarimeter (J-1500, JASCO, Tokyo, Japan) under a constant flow of nitrogen gas. Measurements were performed at room temperature in a quartz cell with a 1 mm path length. The solutions of the S1 protein at 1 μM were prepared in ddH_2O with different concentrations of N1N, R14N, and C15N peptides, respectively. The CD spectra of the S1 protein were recorded between 190 and 260 nm with a scanning speed of 500 nm/min, a spectral bandwidth of 1.0 nm, and a data pitch of 1.0 nm. For each CD spectrum data of the S1 protein, three runs were averaged and corrected by subtracting the contribution of the solvent and peptides at identical concentrations.

4.5. Cell Viability Assay. Cells of 293 T-ACE2$^+$ or A549 were incubated with the peptides at 1 nM, 10 nM, 100 nM, 1 μM, 10 μM, and 100 μM or with the fresh medium as a control group. After 48 h incubation, cells were washed with PBS, and then 100 μL of fresh medium containing 10 μL of CCK-8 reagent was added to each of the wells and incubated at 37 °C. The absorbance value (optical density, OD) was read at 450 and 630 nm and normalized with the control group.

4.6. Western Blot. A549 and 293 T-ACE2$^+$ cells were cultured in 6-well plates. The recombinant SARS-CoV-2 S1 protein was mixed and incubated with peptides at 37 °C for 1 h before being added to the cells. After incubation with cells for 1 h, the cells were washed with PBS, lysed with RIPA (Applygen, Beijing, China), supplemented with PMSF (Solarbio, Beijing, China) and a protein phosphatase inhibitor (Applygen), and then centrifuged at 12,000 rpm at 4 °C for 15 min. After being denatured by boiling in loading buffer (Applygen), an equal amount of protein was loaded and separated by SDS-PAGE, transferred to polyvinylidenedifluoride (PVDF) membranes (0.45 μm; Millipore, Bedford, MA), and blocked with 5% bovine serum albumin (BSA) for 1 h before being probed with specific primary antibodies against ACTB (CST, 8H10D10, Mouse mAb), S1 protein (Sino Biological, Rabbit pAb), and HRP-conjugated secondary anti-mouse and anti-rabbit antibodies (Jackson ImmunoResearch, West Grove, PA). The immune complex on the membrane was visualized using an automatic chemoluminescence image analysis system (Tanon, Shanghai, China) with HRP substrate, luminol reagent, and peroxide solution (Millipore).

4.7. Pseudovirus Affinity and Infection. SARS-CoV-2 pseudovirus was used to test the affinity and the infection blocking effect of peptides to the virus. SARS-CoV-2 pseudovirus was purchased from Genomeditech (Shanghai, China). The pseudovirus expresses the SARS-CoV-2 S protein on the surface and contains a defective HIV-1 genome encoding luciferase and a green fluorescent protein as a reporter; hence, the luciferase and green fluorescent protein (GFP) would be expressed when the pseudovirus enters the host cells.

QCM-D was utilized to determine the affinity of peptides to the pseudovirus. Briefly, the peptides were coated on the gold sensor surfaces and the pseudovirus was applied at a flow rate of 100 μL/min at 37 °C in PBS.

The pseudovirus was also used to test the infection blocking effect of the peptides. Briefly, the pseudovirus was pre-incubated with serially diluted peptides at 37 °C for 1 h before being added to cells. The culture was refreshed with a fresh medium 1 h later and incubated for an additional 47 h. Luciferase activity was measured by a luciferase detecting kit according to the manufacturer's instructions (Promega).

4.8. Statistical Analysis. All data are expressed as mean ± standard error of the mean (SEM). One-way ANOVA was used for statistical analysis and was performed in Graphpad software (v8.0). P-value < 0.05 was considered statistically significant.

■ ASSOCIATED CONTENT

Supporting Information

The Supporting Information is available free of charge at https://pubs.acs.org/doi/10.1021/acs.jmedchem.1c01440.

Purity data of the peptides analyzed by HPLC (PDF)

■ AUTHOR INFORMATION

Corresponding Authors

Chen Wang − *CAS Center for Excellence in Nanoscience, National Center for Nanoscience and Technology, Beijing 100190, China; University of the Chinese Academy of Sciences, Beijing 100049, China*; Email: wangch@nanoctr.cn

Haiyan Xu − *Department of Biomedical Engineering, Institute of Basic Medical Sciences Chinese Academy of Medical Sciences, School of Basic Medicine Peking Union Medical College, Beijing 100005, China*; orcid.org/0000-0002-7287-9048; Email: xuhy@pumc.edu.cn

Authors

Tao Wang − *Department of Biomedical Engineering, Institute of Basic Medical Sciences Chinese Academy of Medical Sciences, School of Basic Medicine Peking Union Medical College, Beijing 100005, China*; orcid.org/0000-0001-7756-9711

Xiaocui Fang − *CAS Center for Excellence in Nanoscience, National Center for Nanoscience and Technology, Beijing*

https://doi.org/10.1021/acs.jmedchem.1c01440
J. Med. Chem. XXXX, XXX, XXX−XXX

100190, China; University of the Chinese Academy of Sciences, Beijing 100049, China

Tao Wen − *Department of Biomedical Engineering, Institute of Basic Medical Sciences Chinese Academy of Medical Sciences, School of Basic Medicine Peking Union Medical College, Beijing 100005, China*

Jian Liu − *Department of Biomedical Engineering, Institute of Basic Medical Sciences Chinese Academy of Medical Sciences, School of Basic Medicine Peking Union Medical College, Beijing 100005, China*

Zhaoyi Zhai − *CAS Center for Excellence in Nanoscience, National Center for Nanoscience and Technology, Beijing 100190, China; University of the Chinese Academy of Sciences, Beijing 100049, China*

Zhiyou Wang − *School of Electric Communication and Electrical Engineering, Changsha University, Changsha 410022, China*

Jie Meng − *Department of Biomedical Engineering, Institute of Basic Medical Sciences Chinese Academy of Medical Sciences, School of Basic Medicine Peking Union Medical College, Beijing 100005, China*

Yanlian Yang − *CAS Center for Excellence in Nanoscience, National Center for Nanoscience and Technology, Beijing 100190, China; University of the Chinese Academy of Sciences, Beijing 100049, China;* orcid.org/0000-0002-5607-5509

Complete contact information is available at: https://pubs.acs.org/10.1021/acs.jmedchem.1c01440

Notes

The authors declare no competing financial interest.

■ ACKNOWLEDGMENTS

We are grateful for helpful discussions from Dr. Jinsong Zhu on analyzing the QCM data. This work was supported by the National Key R&D Program of China (2017YFA0205504), CAMS Innovation Fund for Medical Sciences (CIFMS, 2016-I2M-3-004), the National Natural Science Foundation of China (nos. 51861135103 and 21721002), and the Key Research Program of Frontier Sciences, Chinese Academy of Science (QYZDJ-SSW-SLH048).

■ ABBREVIATIONS

ACE2, angiotensin converting enzyme 2; CD, circular dichroism; COVID-19, coronavirus disease 2019; GFP, green fluorescent protein; PSV, pseudovirus; QCM-D, quartz crystal microbalance with dissipation monitoring; RBD, receptor-binding domain; SARS-CoV-2, severe acute respiratory syndrome coronavirus 2; S protein, Spike protein; SEM, standard error of the mean.

■ REFERENCES

(1) *WHO Coronavirus (COVID-19) Dashboard*; https://covid19.who.int/.

(2) Bedford, J.; Enria, D.; Giesecke, J.; Heymann, D. L.; Ihekweazu, C.; Kobinger, G.; Lane, H. C.; Memish, Z.; Oh, M. D.; Sall, A. A.; Schuchat, A.; Ungchusak, K.; Wieler, L. H. COVID-19: towards controlling of a pandemic. *Lancet* **2020**, *395*, 1015−1018.

(3) Li, Q.; Guan, X.; Wu, P.; Wang, X.; Zhou, L.; Tong, Y.; Ren, R.; Leung, K. S. M.; Lau, E. H. Y.; Wong, J. Y.; Xing, X.; Xiang, N.; Wu, Y.; Li, C.; Chen, Q.; Li, D.; Liu, T.; Zhao, J.; Liu, M.; Tu, W.; Chen, C.; Jin, L.; Yang, R.; Wang, Q.; Zhou, S.; Wang, R.; Liu, H.; Luo, Y.; Liu, Y.; Shao, G.; Li, H.; Tao, Z.; Yang, Y.; Deng, Z.; Liu, B.; Ma, Z.; Zhang, Y.; Shi, G.; Lam, T. T. Y.; Wu, J. T.; Gao, G. F.; Cowling, B. J.; Yang, B.; Leung, G. M.; Feng, Z. Early transmission dynamics in Wuhan, China, of novel coronavirus-infected pneumonia. *N. Engl. J. Med.* **2020**, *382*, 1199−1207.

(4) Zhou, P.; Yang, X. L.; Wang, X. G.; Hu, B.; Zhang, L.; Zhang, W.; Si, H. R.; Zhu, Y.; Li, B.; Huang, C. L.; Chen, H. D.; Chen, J.; Luo, Y.; Guo, H.; Jiang, R. D.; Liu, M. Q.; Chen, Y.; Shen, X. R.; Wang, X.; Zheng, X. S.; Zhao, K.; Chen, Q. J.; Deng, F.; Liu, L. L.; Yan, B.; Zhan, F. X.; Wang, Y. Y.; Xiao, G. F.; Shi, Z. L. A pneumonia outbreak associated with a new coronavirus of probable bat origin. *Nature* **2020**, *579*, 270−273.

(5) Vabret, N.; Britton, G. J.; Gruber, C.; Hegde, S.; Kim, J.; Kuksin, M.; Levantovsky, R.; Malle, L.; Moreira, A.; Park, M. D.; Pia, L.; Risson, E.; Saffern, M.; Salomé, B.; Esai Selvan, M.; Spindler, M. P.; Tan, J.; van der Heide, V.; Gregory, J. K.; Alexandropoulos, K.; Bhardwaj, N.; Brown, B. D.; Greenbaum, B.; Gümüş, Z. H.; Homann, D.; Horowitz, A.; Kamphorst, A. O.; Curotto de Lafaille, M. A.; Mehandru, S.; Merad, M.; Samstein, R. M.; Sinai Immunology Review Project. Immunology of COVID-19: current state of the science. *Immunity* **2020**, *52*, 910−941.

(6) Lan, J.; Ge, J.; Yu, J.; Shan, S.; Zhou, H.; Fan, S.; Zhang, Q.; Shi, X.; Wang, Q.; Zhang, L.; Wang, X. Structure of the SARS-CoV-2 spike receptor-binding domain bound to the ACE2 receptor. *Nature* **2020**, *581*, 215−220.

(7) Kaur, S. P.; Gupta, V. COVID-19 Vaccine: A comprehensive status report. *Virus Res.* **2020**, *288*, 198114.

(8) Wang, M.; Cao, R.; Zhang, L.; Yang, X.; Liu, J.; Xu, M.; Shi, Z.; Hu, Z.; Zhong, W.; Xiao, G. Remdesivir and chloroquine effectively inhibit the recently emerged novel coronavirus (2019-nCoV) in vitro. *Cell Res.* **2020**, *30*, 269−271.

(9) Wrapp, D.; Wang, N.; Corbett, K. S.; Goldsmith, J. A.; Hsieh, C. L.; Abiona, O.; Graham, B. S.; McLellan, J. S. Cryo-EM structure of the 2019-nCoV spike in the prefusion conformation. *Science* **2020**, *367*, 1260−1263.

(10) Zeng, Q.; Huang, G.; Li, Y. Z.; Xu, Y. Tackling COVID19 by exploiting pre-existing cross-reacting spike-specific immunity. *Mol. Ther.* **2020**, *28*, 2314−2315.

(11) Lv, H.; Wu, N. C.; Tsang, O. T.-Y.; Yuan, M.; Perera, R. A. P. M.; Leung, W. S.; So, R. T. Y.; Chan, J. M. C.; Yip, G. K.; Chik, T. S. H.; Wang, Y.; Choi, C. Y. C.; Lin, Y.; Ng, W. W.; Zhao, J.; Poon, L. L. M.; Peiris, J. S. M.; Wilson, I. A.; Mok, C. K. P. Cross-reactive antibody response between SARS-CoV-2 and SARS-CoV infections. *Cell Rep.* **2020**, *31*, 107725.

(12) Yuan, M.; Wu, N. C.; Zhu, X.; Lee, C.-C. D.; So, R. T. Y.; Lv, H.; Mok, C. K. P.; Wilson, I. A. A highly conserved cryptic epitope in the receptor binding domains of SARS-CoV-2 and SARS-CoV. *Science* **2020**, *368*, 630−633.

(13) Baum, A.; Fulton, B. O.; Wloga, E.; Copin, R.; Pascal, K. E.; Russo, V.; Giordano, S.; Lanza, K.; Negron, N.; Ni, M.; Wei, Y.; Atwal, G. S.; Murphy, A. J.; Stahl, N.; Yancopoulos, G. D.; Kyratsous, C. A. Antibody cocktail to SARS-CoV-2 spike protein prevents rapid mutational escape seen with individual antibodies. *Science* **2020**, *369*, 1014−1018.

(14) Li, Y.; Lai, D. Y.; Zhang, H. N.; Jiang, H. W.; Tian, X.; Ma, M. L.; Qi, H.; Meng, Q. F.; Guo, S. J.; Wu, Y.; Wang, W.; Yang, X.; Shi, D. W.; Dai, J. B.; Ying, T.; Zhou, J.; Tao, S. C. Linear epitopes of SARS-CoV-2 spike protein elicit neutralizing antibodies in COVID-19 patients. *Cell Mol. Immunol.* **2020**, *17*, 1095−1097.

(15) Weinreich, D. M.; Sivapalasingam, S.; Norton, T.; Ali, S.; Gao, H.; Bhore, R.; Musser, B. J.; Soo, Y.; Rofail, D.; Im, J.; Perry, C.; Pan, C.; Hosain, R.; Mahmood, A.; Davis, J. D.; Turner, K. C.; Hooper, A. T.; Hamilton, J. D.; Baum, A.; Kyratsous, C. A.; Kim, Y.; Cook, A.; Kampman, W.; Kohli, A.; Sachdeva, Y.; Graber, X.; Kowal, B.; DiCioccio, T.; Stahl, N.; Lipsich, L.; Braunstein, N.; Herman, G.; Yancopoulos, G. D.; Trial Investigators. REGN-COV2, a neutralizing antibody cocktail, in outpatients with Covid-19. *N. Engl. J. Med.* **2021**, *384*, 238−251.

(16) Gottlieb, R. L.; Nirula, A.; Chen, P.; Boscia, J.; Heller, B.; Morris, J.; Huhn, G.; Cardona, J.; Mocherla, B.; Stosor, V.; Shawa, I.;

Kumar, P.; Adams, A. C.; Van Naarden, J.; Custer, K. L.; Durante, M.; Oakley, G.; Schade, A. E.; Holzer, T. R.; Ebert, P. J.; Higgs, R. E.; Kallewaard, N. L.; Sabo, J.; Patel, D. R.; Klekotka, P.; Shen, L.; Skovronsky, D. M. Effect of Bamlanivimab as monotherapy or in combination with etesevimab on viral load in patients with mild to moderate COVID-19: a randomized clinical trial. *J. Am. Med. Assoc.* **2021**, *325*, 632−644.

(17) Chi, X.; Liu, X.; Wang, C.; Zhang, X.; Li, X.; Hou, J.; Ren, L.; Jin, Q.; Wang, J.; Yang, W. Humanized single domain antibodies neutralize SARS-CoV-2 by targeting the spike receptor binding domain. *Nat. Commun.* **2020**, *11*, 4528.

(18) Lei, C.; Qian, K.; Li, T.; Zhang, S.; Fu, W.; Ding, M.; Hu, S. Neutralization of SARS-CoV-2 spike pseudotyped virus by recombinant ACE2-Ig. *Nat. Commun.* **2020**, *11*, 2070.

(19) de Vries, R. D.; Schmitz, K. S.; Bovier, F. T.; Predella, C.; Khao, J.; Noack, D.; Haagmans, B. L.; Herfst, S.; Stearns, K. N.; Drew-Bear, J.; Biswas, S.; Rockx, B.; McGill, G.; Dorrello, N. V.; Gellman, S. H.; Alabi, C. A.; de Swart, R. L.; Moscona, A.; Porotto, M. Intranasal fusion inhibitory lipopeptide prevents direct-contact SARS-CoV-2 transmission in ferrets. *Science* **2021**, *371*, 1379−1382.

(20) Du, H.; Hu, X.; Duan, H.; Yu, L.; Qu, F.; Huang, Q.; Zheng, W.; Xie, H.; Peng, J.; Tuo, R.; Yu, D.; Lin, Y.; Li, W.; Zheng, Y.; Fang, X.; Zou, Y.; Wang, H.; Wang, M.; Weiss, P. S.; Yang, Y.; Wang, C. Principles of inter-amino-acid recognition revealed by binding energies between homogeneous oligopeptides. *ACS Central Sci.* **2019**, *5*, 97−108.

(21) Bai, L.; Du, Y.; Peng, J.; Liu, Y.; Wang, Y.; Yang, Y.; Wang, C. Peptide-based isolation of circulating tumor cells by magnetic nanoparticles. *J. Mater. Chem. B* **2014**, *2*, 4080−4088.

(22) Li, X.; Guo, H.; Yang, Y.; Meng, J.; Liu, J.; Wang, C.; Xu, H. A designed peptide targeting CXCR4 displays anti-acute myelocytic leukemia activity in vitro and in vivo. *Sci. Rep.* **2015**, *4*, 1.

(23) Li, X.; Guo, H.; Duan, H.; Yang, Y.; Meng, J.; Liu, J.; Wang, C.; Xu, H. Improving chemotherapeutic efficiency in acute myeloid leukemia treatments by chemically synthesized peptide interfering with CXCR4/CXCL12 axis. *Sci. Rep.* **2015**, *5*, 1.

(24) Zheng, Y.; Fang, X.; Yang, Y.; Wang, C. Peptide-directed delivery of drug-loaded nanocarriers targeting CD36 overexpressing cells. *Colloids Surf., A* **2021**, *610*, 125970.

(25) Bulheller, B. M.; Rodger, A.; Hirst, J. D. Circular and linear dichroism of proteins. *Phys. Chem. Chem. Phys.* **2007**, *9*, 2020−2035.

(26) Ranjbar, B.; Gill, P. Circular dichroism techniques: biomolecular and nanostructural analyses- a review. *Chem. Biol. Drug Des.* **2009**, *74*, 101−120.

(27) Kojima, S.; Kuriki, Y.; Sato, Y.; Arisaka, F.; Kumagai, I.; Takahashi, S.; Miura, K. Synthesis of alpha-helix-forming peptides by gene engineering methods and their characterization by circular dichroism spectra measurements. *Biochim. Biophys. Acta* **1996**, *1294*, 129−137.

(28) Avitabile, C.; D'Andrea, L. D.; Romanelli, A. Circular Dichroism studies on the interactions of antimicrobial peptides with bacterial cells. *Sci. Rep.* **2015**, *4*, 4293.

(29) Duan, H.; Zhu, L.; Hou, J.; Peng, J.; Xie, H.; Lin, Y.; Liu, C.; Li, W.; Xu, H.; Wang, C.; Yang, Y. Dual-affinity peptide mediated inter-protein recognition. *Org. Biomol. Chem.* **2016**, *14*, 11342−11346.

(30) Rózga, M.; Kłoniecki, M.; Jabłonowska, A.; Dadlez, M.; Bal, W. The binding constant for amyloid Abeta40 peptide interaction with human serum albumin. *Biochem. Biophys. Res. Commun.* **2007**, *364*, 714−718.

(31) Kulkarni, P. M.; Kulkarni, A. R.; Korde, A.; Tichkule, R. B.; Laprairie, R. B.; Denovan-Wright, E. M.; Zhou, H.; Janero, D. R.; Zvonok, N.; Makriyannis, A.; Cascio, M. G.; Pertwee, R. G.; Thakur, G. A. Novel electrophilic and photoaffinity covalent probes for mapping the cannabinoid 1 receptor allosteric site(s). *J. Med. Chem.* **2016**, *59*, 44−60.

(32) Lane, J. R.; Abdul-Ridha, A.; Canals, M. Regulation of G protein-coupled receptors by allosteric ligands. *ACS Chem. Neurosci.* **2013**, *4*, 527−534.

(33) Dokholyan, N. V. Controlling allosteric networks in proteins. *Chem. Rev.* **2016**, *116*, 6463−6487.

(34) Gruber, R.; Horovitz, A. Allosteric mechanisms in chaperonin machines. *Chem. Rev.* **2016**, *116*, 6588−6606.

(35) Qi, Y.; Wang, Q.; Tang, B.; Lai, L. Identifying allosteric binding sites in proteins with a two-state gō model for novel allosteric effector discovery. *J. Chem. Theory Comput.* **2012**, *8*, 2962−2971.

(36) Liu, J.; Zheng, X.; Tong, Q.; Li, W.; Wang, B.; Sutter, K.; Trilling, M.; Lu, M.; Dittmer, U.; Yang, D. Overlapping and discrete aspects of the pathology and pathogenesis of the emerging human pathogenic coronaviruses SARS-CoV, MERS-CoV, and 2019-nCoV. *J. Med. Virol.* **2020**, *92*, 491−494.

(37) Abbott, T. R.; Dhamdhere, G.; Liu, Y.; Lin, X.; Goudy, L.; Zeng, L.; Chemparathy, A.; Chmura, S.; Heaton, N. S.; Debs, R.; Pande, T.; Endy, D.; La Russa, M. F.; Lewis, D. B.; Qi, L. S. Development of CRISPR as an antiviral strategy to combat SARS-CoV-2 and influenza. *Cell* **2020**, *181*, 865−876.e12.

(38) Ju, B.; Zhang, Q.; Ge, J.; Wang, R.; Sun, J.; Ge, X.; Yu, J.; Shan, S.; Zhou, B.; Song, S.; Tang, X.; Yu, J.; Lan, J.; Yuan, J.; Wang, H.; Zhao, J.; Zhang, S.; Wang, Y.; Shi, X.; Liu, L.; Zhao, J.; Wang, X.; Zhang, Z.; Zhang, L. Human neutralizing antibodies elicited by SARS-CoV-2 infection. *Nature* **2020**, *584*, 115−119.

(39) Cao, Y.; Su, B.; Guo, X.; Sun, W.; Deng, Y.; Bao, L.; Zhu, Q.; Zhang, X.; Zheng, Y.; Geng, C.; Chai, X.; He, R.; Li, X.; Lv, Q.; Zhu, H.; Deng, W.; Xu, Y.; Wang, Y.; Qiao, L.; Tan, Y.; Song, L.; Wang, G.; Du, X.; Gao, N.; Liu, J.; Xiao, J.; Su, X. D.; Du, Z.; Feng, Y.; Qin, C.; Qin, C.; Jin, R.; Xie, X. S. Potent neutralizing antibodies against SARS-CoV-2 identified by high-throughput single-cell sequencing of convalescent patients' B Cells. *Cell* **2020**, *182*, 73−84.e16.

(40) Chi, X.; Yan, R.; Zhang, J.; Zhang, G.; Zhang, Y.; Hao, M.; Zhang, Z.; Fan, P.; Dong, Y.; Yang, Y.; Chen, Z.; Guo, Y.; Zhang, J.; Li, Y.; Song, X.; Chen, Y.; Xia, L.; Fu, L.; Hou, L.; Xu, J.; Yu, C.; Li, J.; Zhou, Q.; Chen, W. A neutralizing human antibody binds to the N-terminal domain of the Spike protein of SARS-CoV-2. *Science* **2020**, *369*, 650−655.

(41) Liu, L.; Wang, P.; Nair, M. S.; Yu, J.; Rapp, M.; Wang, Q.; Luo, Y.; Chan, J. F.-W.; Sahi, V.; Figueroa, A.; Guo, X. V.; Cerutti, G.; Bimela, J.; Gorman, J.; Zhou, T.; Chen, Z.; Yuen, K. Y.; Kwong, P. D.; Sodroski, J. G.; Yin, M. T.; Sheng, Z.; Huang, Y.; Shapiro, L.; Ho, D. D. Potent neutralizing antibodies against multiple epitopes on SARS-CoV-2 spike. *Nature* **2020**, *584*, 450−456.

(42) Cohen, M. S. Monoclonal antibodies to disrupt progression of early Covid-19 Infection. *N. Engl. J. Med.* **2021**, *384*, 289−291.

https://doi.org/10.1021/acs.jmedchem.1c01440
J. Med. Chem. XXXX, XXX, XXX−XXX